Multi-step and anomalous reproducible behaviour of the electrical resistivity near the first-order magnetostructural transition of $Gd_5(Si_{0.1}Ge_{0.9})_4$

2005 J. Phys.: Condens. Matter 17 2461

(http://iopscience.iop.org/0953-8984/17/15/017)

INSTITUTE OF PHYSICS PUBLISHING JOURNAL OF PHYSICS: CONDENSED MATTER

J. Phys.: Condens. Matter **17** (2005) 2461–2476 doi:10.1088/0953-8984/17/15/017

Multi-step and anomalous reproducible behaviour of the electrical resistivity near the first-order magnetostructural transition of $Gd_5(Si_{0.1}Ge_{0.9})_4$

J B Sousa[1], A M Pereira[1], F C Correia[1], J M Teixeira[1], J P Araújo[1], R P Pinto[1], M E Braga[1], L Morellon[2], P A Algarabel[2], C Magen[2] and M R Ibarra[2]

[1] IFIMUP and Physics Department of FCUP, University of Porto, R Campo Alegre 687, Porto 4169-007, Portugal
[2] Departamento de Física de la Materia Condensada and Instituto de Ciencia de Materiales de Aragón, Universidad de Zaragoza and Consejo Superior de Investigaciones Científicas, 50009 Zaragoza, Spain

E-mail: jbsousa@fc.up.pt

Received 30 August 2004, in final form 4 February 2005
Published 1 April 2005
Online at stacks.iop.org/JPhysCM/17/2461

Abstract

Very detailed measurements of the electrical resistivity of $Gd_5(Si_{0.1}Ge_{0.9})_4$ are here reported, with special emphasis on the vicinity of the first-order (magnetostructural) martensitic transition which occurs at $T_S \sim 87$ K. The data cover more than fifty thermal cycles spanning the temperature ranges of 300–10 K (long cycles) and 105–10 K (short cycles). In the initial 10–300 K cycles the martensitic transition takes place in three closely-spaced steps, with associated resistance (R) discontinuities and large thermal hysteresis. In a subsequent series of short cycles (10–105 K) a unique transition occurs, exhibiting a common and quite reproducible $R(T)$ behaviour within a small temperature range ($\Delta T \sim 4$ K) below T_S, either in heating or cooling runs. Remarkably, this 'local reproducibility' (within ΔT) remains in spite of the significant resistance changes which occur outside the ΔT-range under thermal cycling. In particular the residual resistance systematically increases under thermal cycling, but the corresponding effect is absent in the ΔT temperature range. This excludes microcracking as a dominant resistive mechanism in our results, pointing to an intrinsic character of the reproducible behaviour just below T_S. We also analyse the $R(T)$ behaviour when changing from long to short thermal cycles, and the $R(T)$ evolution towards a reversible final behaviour, after extended thermal cycling.

1. Introduction

The giant magnetocaloric $Gd_5(Si_xGe_{1-x})_4$ system has been intensively studied due to its unusual magnetostructural transitions and potential for technological applications, namely in magnetic refrigeration [1–6]. The corresponding phase diagram has been established, both as a function of composition and temperature [7, 8]. The nanoscopic layered structure of these compounds (formed by parallel slabs of atoms) plays an important role in their physical properties. Each slab is formed by five atomic planes (Si, Ge/Gd/Gd, Si, Ge/Gd/Si, Ge) tightly bonded together to about 0.6 nm thickness [1]. Covalent pairs of Si (or Ge) atoms form between the outer atomic planes of neighbouring slabs at low temperatures, producing strong interslab bonding and leading to the so-called orthorhombic O(I) phase. Upon heating, a martensitic-like transition can occur (at T_S), producing opposite sliding of neighbouring slabs with the total or partial breaking of the covalent pairs mentioned [9], and the onset of other crystallographic phases.

Three structural phases are possible in the $Gd_5(Si_xGe_{1-x})_4$ compounds at room temperature [7, 8, 10]. For $x > 0.58$, the compounds have the orthorhombic Gd_5Si_4-type structure (O(I)), with all the interslab bonds formed. For $0.4 \leqslant x \leqslant 0.5$, the compounds have a monoclinic structure (M), where only half of the interslab bonds remain. For $x \leqslant 0.3$, one has the orthorhombic Sm_5Ge_4 structure (O(II)), with no interslab covalent bonds.

All compounds are paramagnetic (PM) at room temperature. Under cooling, the $x > 0.58$ compounds (initially O(I), PM) become ferromagnetic (FM) without any structural transition, and the Curie temperature T_C is only weakly dependent on composition. For the $0.4 \leqslant x \leqslant 0.5$ compounds (M, PM), a first-order magnetostructural transition to an (O(I), FM) phase occurs at a critical point T_S through martensitic displacements, reconstructing all the inter-slab covalent bonds. For the $x \leqslant 0.3$ compounds (O(II), PM) a second-order magnetic transition first takes place, from the PM to an antiferromagnetic-like phase (AFM*, $T < T_N$) and without structural changes. At a lower temperature T_S, a first-order magnetostructural transition occurs producing the (O(I), FM) phase, where all interslab bonds are reconstructed through martensitic displacements [11].

The general features of the electrical resistance (R) and dR/dT of $Gd_5(Si_{0.1}Ge_{0.9})_4$ under thermal cycling between 10 and 300 K were previously published [12]. Here we report a much more comprehensive study of $R(T)$ with special emphasis on the behaviour in the vicinity of the magnetostructural transition (T_S), under different conditions of thermal cycling.

Our study reveals various types of $R(T)$ behaviour near T_S. In the initial 10–300 K cycles (11 complete cycles) the martensitic transition occurs in multiple steps at slightly different temperatures, causing discontinuities in R and large thermal hysteresis.

In a subsequent series of shorter thermal cycles (10–105 K) a unique martensitic step is observed in each $R(T)$ curve (heating or cooling), but large thermal hysteresis remains. However, it is remarkable that within a small ΔT-range below T_S ($\approx$4 K) the $R(T)$-values become significantly different (high resistive state) from those above and below and, moreover, they are virtually the same irrespective of heating or cooling runs (strict reproducible behaviour). This kind of 'local universality' in such a high resistive state remains in spite of the significant increase of the residual resistance (and of R above T_S) under thermal cycling. Further cycling enhances $R(T)$ above T_S, with its values approaching those observed within ΔT below T_S (high-resistivity phase) leading to a pronounced decrease in thermal hysteresis. Ultimately a quasi-reversible $R(T)$ dependence signals the onset of well defined and reproducible phases over the whole temperature range, after sufficient thermal cycling.

2. Experimental details

The $Gd_5(Si_{0.1}Ge_{0.9})_4$ compound was synthesized by arc melting of 99.9 wt% pure Gd and 99.9999 wt% pure Si and Ge under a high-purity argon atmosphere. The initial composition was assumed unchanged; the quality of the sample was checked by scanning electron microscopy and x-ray diffraction at room temperature. The measurements confirmed the presence of an orthorhombic main phase with unit-cell parameters $a = 7.6887(1)$ Å, $b = 14.827(2)$ Å and $c = 7.7785(1)$ Å [8]. A small amount of a secondary phase was detected and indexed as hexagonal $Gd_5(Si, Ge)_3$. The sample studied here corresponds to sample A1 in [12] (cross-section: 0.7×1.2 mm^2; length: 1.8 mm), and was mounted in a temperature-controlled copper basis in an He closed cycle cryostat. A four-point potentiometric method was used to measure the electrical resistivity, as described in [13]. The data reported in this work were obtained under 0.5 K min^{-1} heating or cooling rates. The effect of different heating rates on the $R(T)$ behaviour was studied using quasi-static (0.05 K min^{-1}) as well as 1.5 K min^{-1} rates. Within the experimental errors, we did not observe any relevant changes attributable to the different rates used. Possible temperature gradients along the sample were negligible, as the sample was directly glued on a massive copper block using a thin layer of GE-varnish. For a temperature rate of 0.5 K min^{-1} (with the sample glued on the copper block central region, under symmetric cooling/heating conditions) and a 4 mm sample length, the maximum (estimated) temperature difference along the sample is below 0.05 K.

3. Experimental results

This paper focuses on the study of $R(T)$ near T_S in a $Gd_5(Si_{0.1}Ge_{0.9})_4$ sample (A1), along different series of 10–105 or 10–300 K thermal cycles, with measurements in the cooling and heating runs. We will use the symbol p to specify a particular thermal cycle. Each series described below contains consecutive runs performed under the same conditions, i.e. thermal runs performed under different conditions separate different series.

Sample A1 of $Gd_5(Si_{0.1}Ge_{0.9})_4$ was previously subjected to eight 10–300 K thermal cycles before the systematic study of $R(T)$ here presented. The general features of the electrical resistivity and dR/dT in such earlier runs was reported in [12]. Essentially, a sharp peak occurred in the electrical resistivity near the first-order magnetostructural transition (T_S), with pronounced thermal hysteresis, whereas a smooth (second-order) magnetic transition was observed at the Néel temperature T_N, as shown in figure 1 taken from [12]. Subsequent re-inspection of such resistivity data using an expanded scale near T_S (not done in [12]), effectively revealed a transition split into several steps, separated by a few degrees, as illustrated for the fourth cooling run in the inset of figure 1. These new features motivated the present detailed study of $R(T)$ near T_S, under different conditions of cycling. The thermal evolution of the sample along the different series of runs reported in this paper ($p = 9$–50) and also in the previous work ($p = 1$–8; [12]) is given in figure 2.

3.1. Series 1 (runs 9–12)

This series started with the ninth cooling run, from 300 to 10 K (figure 2(b)). As can be seen in figure 3(a), the first-order magnetostructural transition occurs in three steps, associated with discontinuous resistance increases (ΔR_i). The magnitude of the steps and the absolute $R(T)$-values change from run to run (9–12), but the i-steps occur approximately at the same temperatures ($T_i = 84.8$, 83.4 and 80.8 K). In these cooling runs the high-temperature phase ($T > T_S$, where T_S is identified with the highest observed T_i) has a smaller resistance than

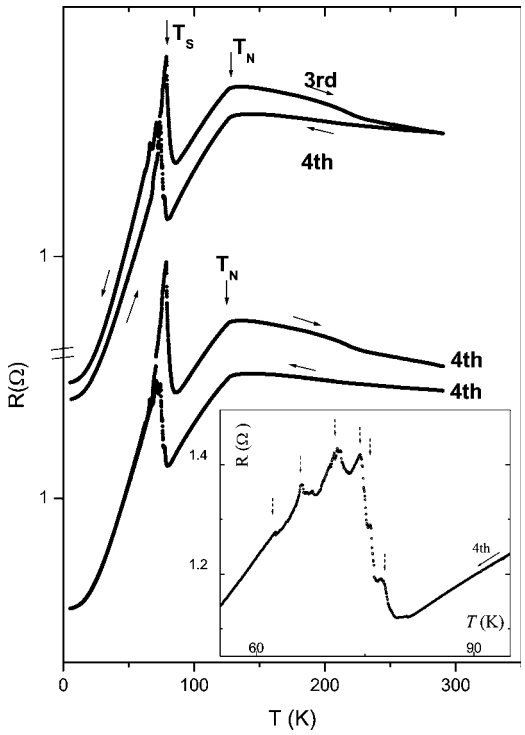

Figure 1. Temperature dependence of the electrical resistivity of $Gd_5(Si_{0.1}Ge_{0.9})_4$ (sample A in [12]) for the heating run 3 and fourth cooling/heating runs (10–300 K). Inset: expanded scale illustrating the temperature dependence of the electrical resistivity in the fourth cooling run, from 55 to 95 K.

the low-temperature phase (see also figure 4(a)) and the residual resistance systematically increases under cycling.

Under *heating* (figure 3(b)) the three ΔR_i-anomalies occur at temperatures $\simeq$2 K higher than in the cooling runs, but the (two) anomalies below T_S become less defined. The R-values also systematically increase from run to run over the whole temperature range. On the other hand fair extrapolation occurs between $R(T)$ below $\sim$80 K and just after T_S (see the dashed line in figure 3(b), run 9), which contrasts with the cooling case.

To illustrate thermal hysteresis, figure 4 compares $R(T)$ in two consecutive ($p = 11$ cooling/heating) runs. The hysteresis is large near and above T_S, but virtually disappears below $T^* \simeq 58$ K for the particular runs displayed.

3.2. Series 2 (runs 12–21)

A new $R(T)$ behaviour suddenly appears in the 12th heating run, as shown in the bottom curve of figure 5(b) (also see the inset). Instead of the previous succession of three ΔR_i anomalies (figure 3(b)), a unique and large R increase occurs at a temperature $T_\Delta \simeq 85.5$ K, followed by an equally large and very sharp R decrease at $T_S \simeq 87.0$ K. A temperature range of high resistivity thus exists between 85.5 and 87.0 K, just before the magnetostructural transition.

The extreme $R(T)$ sharpness observed at T_S in all the runs described (9–12), and the sudden change in the $R(T)$ behaviour below T_S observed in run 12, rules out chemical inhomogeneities as a possible cause for the three-step transition previously observed (figures 3 and 4; also observed in runs $p < 9$, [12]). For later consideration, we mention that the (totally different)

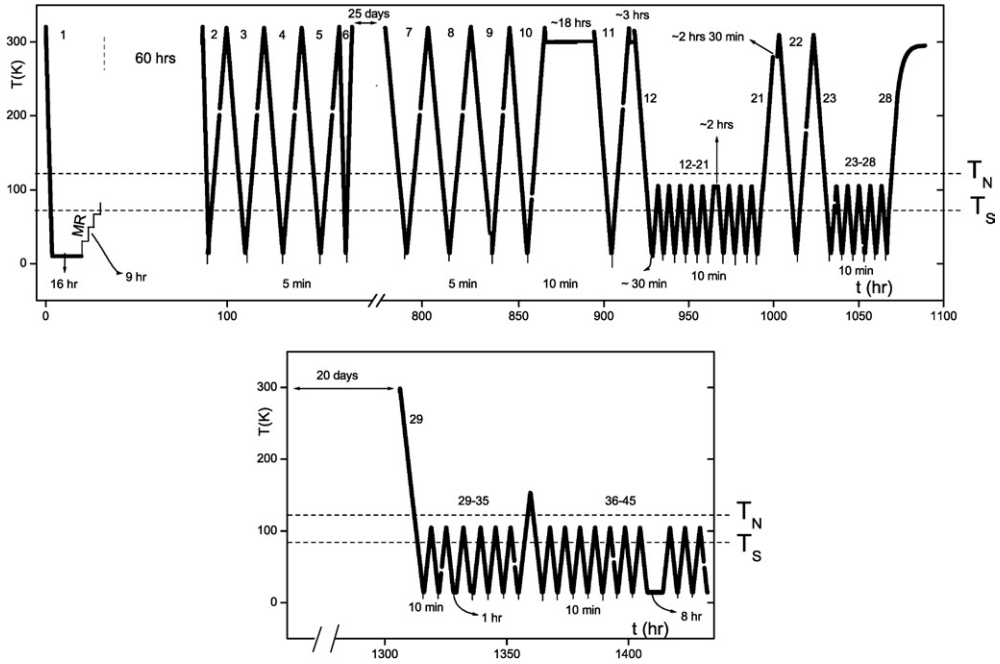

Figure 2. Time dependence of the thermal evolution of the $Gd_5(Si_{0.1}Ge_{0.9})_4$ sample reported in this paper (runs 9–45) and in [12] (runs 1–8). The first heating run was devoted to magnetoresistance measurements (MR), at several static temperatures between 4 and 80 K (9 h). A 3 h warming period followed until room temperature. The sample then remained 60 h before the next run (second). The zig-zag lines in the different thermal cycles typically correspond to heating/cooling rates of 0.5 K min^{-1} (see section 2).

12th heating run was preceded by the following thermal sequence: sample maintained at 300 K for 3 h (after the 11th heating run), then cooled to 10 K under 0.5 K min^{-1} (12th cooling run) and maintained at 10 K for 30 min. After this waiting period before resuming the $R(T)$ measurements, the resistance value had decreased ∼20%, from 4.21 to 3.51 Ω (see the inset of figure 5(b)).

To investigate such an unexpected feature in great detail, we performed a series of shorter thermal cycles (10–105 K) through T_S, ensuring that the sample did not reach the magnetic transition at T_N [12]. Accordingly, the anomalous heating run (12th) was stopped at 105 K. The subsequent short-cycle results are shown in figures 5(a) (cooling runs 13–15, 17, 19 and 21) and (b) (heating runs 13–15, 17, 19 and 21).

Under cooling from 105 K (figure 5(a)) R decreases smoothly until $T_S \simeq 84.4$ K, where a sharp increase in resistance signals the first-order magnetostructural transition. Remarkably, in spite of the quite different starting R-values at 105 K in successive runs, $R(T)$ always merges into a common curve immediately below T_S. This reproducible behaviour is however localized, as it only persists down to a run-dependent temperature T_Δ, where a sudden resistance decrease occurs, suggesting a well defined transition point. We notice that the ΔT region of 'local reproducibility', $(T_S - T_\Delta)$, grows considerably with cycling, e.g. $\Delta T \simeq 2, 6.5$ and 11 K in the cooling runs 13, 15 and 21 respectively, essentially reflecting the significant decrease of T_Δ with thermal cycling (only a small increase is observed in T_S).

In the *heating runs* (figure 5(b)) the T_S and T_Δ transitions also occur, but with a smaller ΔT-range of reproducibility under thermal cycling. In fact T_S remains virtually constant

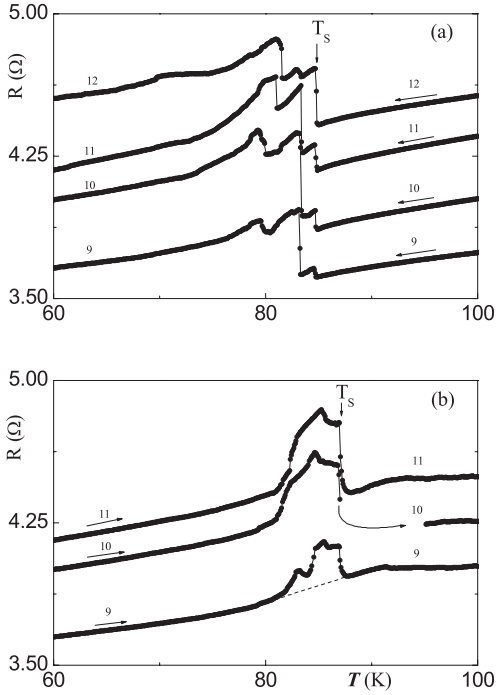

Figure 3. (a) Temperature dependence of the electrical resistance in four *cooling* runs ($p = 9$–12h) from 300–10 K; (b) corresponding data obtained in the alternating *heating* runs (9–11; 10–300 K). The dashed line is a guide to the eye.

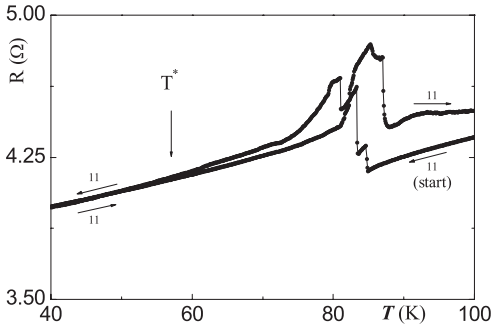

Figure 4. Temperature dependence $R(T)$ of $Gd_5(Si_{0.1}Ge_{0.9})_4$ in the 11th cooling and heating runs (10–300 K).

($T_S \simeq 87$ K), whereas T_Δ only decreases slightly, giving $\Delta T = 2.0$, 2.8 and 3.2 K in the heating runs 12, 15 and 21 respectively.

The thermal hysteresis, T_S(heating)–T_S(cooling), decreases slightly under cycling, corresponding to $\Delta T_S = 2.3$, 2.0 and 1.8 K in runs 12, 15 and 21, respectively. We also notice that the T_Δ transition under heating is always very sharp (first-order-like; figure 5(b)) whereas under cooling it evolves rapidly to second order (figure 5(a)).

In spite of all the effects mentioned above and the $R(T)$ changes with cycling, we always observe the *same* R-values (to better than $1{:}10^2$) within the ΔT-range below T_S, indicating an entirely reproducible magneto-structural state immediately below T_S. A better view can

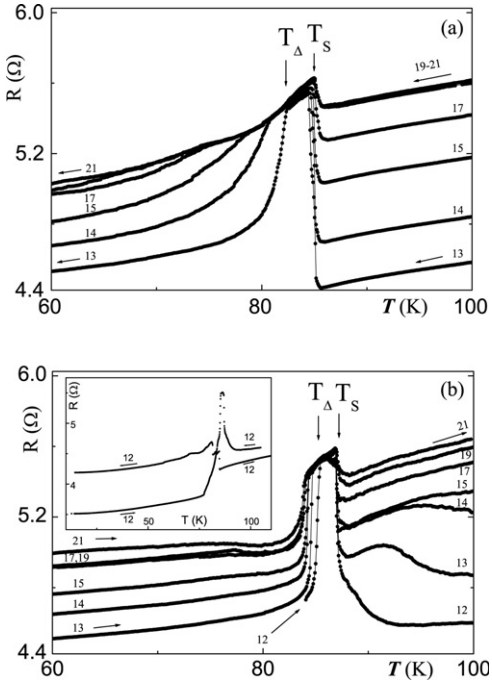

Figure 5. (a) Temperature dependence $R(T)$ in $Gd_5(Si_{0.1}Ge_{0.9})_4$, in cooling runs 13–15, 17, 19 and 21 (105–10 K). (b) $R(T)$ in heating runs 13–15, 17, 19 and 21 (10–105 K). Inset: extended temperature dependence $R(T)$ in the 12th run (cooling/heating), where the $R(T)$ behaviour changed dramatically.

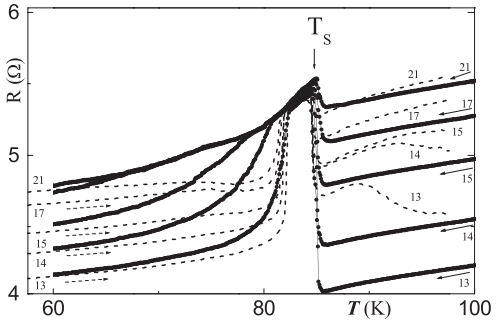

Figure 6. Comparison of the temperature dependence $R(T)$ in the cooling (heavy curve) and heating (dashed curve) runs 13–15, 17 and 21 for $Gd_5(Si_{0.1}Ge_{0.9})_4$, with a 2.3 K temperature shift (downwards) in the heating run results.

be obtained if we plot the cooling and the heating $R(T)$ curves in the same graph, but with a 2.3 K shift (downwards) in the heating curves (figure 6), to account for the ΔT_S hysteresis. For further reference the common behaviour within the ΔT-range will be termed by $R_u(T)$ (reproducible from run to run).

A detailed view of the $R(T)$ hysteresis in short thermal cycles (10–105 K) is displayed in figures 7(a) and (b), for the 13th and 16th cooling/heating runs, respectively. In agreement with our previous remarks, the heating curves do not change much from the 13th to the 16th runs,

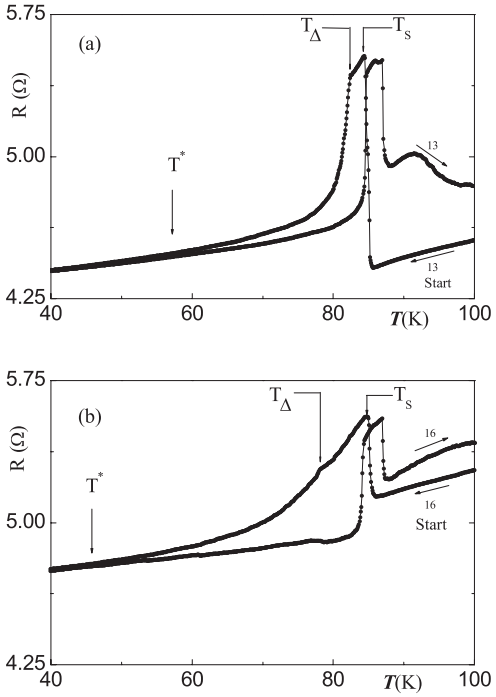

Figure 7. (a) Temperature dependence $R(T)$ in $Gd_5(Si_{0.1}Ge_{0.9})_4$, for the 13th cooling and heating runs. (b) $R(T)$ for the 16th cooling and heating runs.

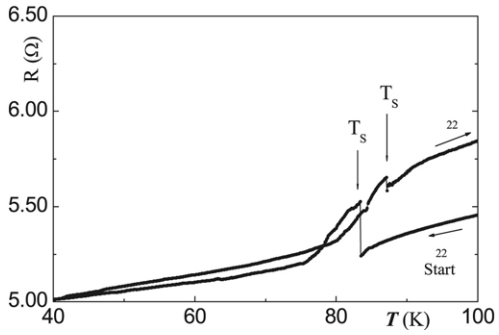

Figure 8. Temperature dependence $R(T)$ obtained for $Gd_5(Si_{0.1}Ge_{0.9})_4$ in the 22nd cooling (300–10 K) and heating runs (10–300 K).

but the cooling curves show a pronounced lowering of T_Δ and a reduction in the sharpness of the associated transition. Furthermore, the effects of such a transition extend well below T_Δ, to about $T^* = 57.3$ and 45.8 K (cooling runs 13 and 16, respectively), where thermal hysteresis disappears.

After the described 10–105 K thermal cycles (12–21), the sample was warmed to 300 K, staying at this temperature for 2 h 30 min (see figure 2), and then a 10–300 K cycle followed (run 22). The previous qualitative $R(T)$ behaviour (cooling versus heating curves) was disrupted by such a thermal cycle, as shown in figure 8. In the cooling run one still observes a large resistance increase at $T \approx T_S$ (as in cooling run 16; figure 7(b)), but in the subsequent heating run only a

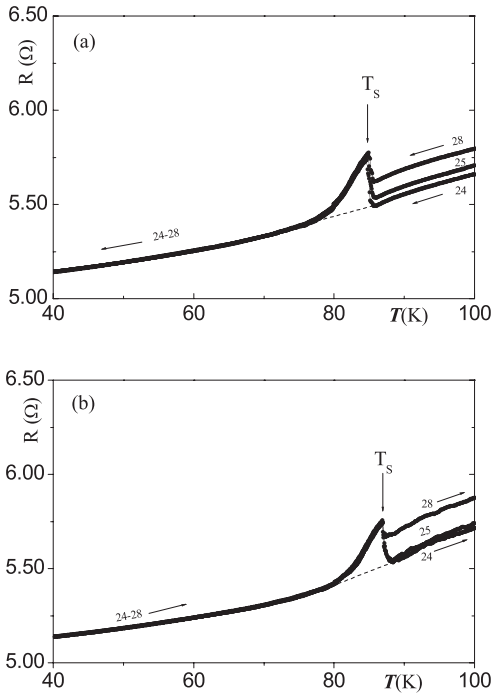

Figure 9. (a) Temperature dependence $R(T)$ in $Gd_5(Si_{0.1}Ge_{0.9})_4$ obtained in the 24–28th cooling runs (105–10 K). (b) $R(T)$ in the 24–28th heating runs (10–105 K). The dashed line is a guide to the eye.

small R decrease occurs at T_S resulting in a high resistance phase at higher temperatures. Also, the sharp R increase previously observed under heating at T_Δ (see figure 6(b)) is now absent and $R(T)$ gradually rises from low temperatures to T_S. This resembles the cooling $R(T)$ trend below T_S, as if a common qualitative $R(T)$ behaviour is being reached in both cases. The new $R(T)$ dependence remains in a subsequent 300–10–105 K cycle ($p = 23$; not shown), after which we again performed several 10–105 K thermal cycles, as described in the next section.

3.3. Series 3 (runs 24–28)

The $R(T)$ behaviour in the 10–105 K cooling and heating runs 24–28 is shown in figures 9(a) and (b), respectively. The magnetostructural transition continues to occur in a single stage and the $R(T)$ curves are virtually the same below T_S for cooling and heating runs, in spite of some differences above T_S.

Thermal hysteresis in the magnetostructural transition point amounts now to $\Delta T_S \simeq 2.0$ K. If one shifts by this ΔT_S the temperature scale of one type of the runs, a common $R(T)$ curve emerges all the way *below* T_S (figure 10), but not above. These results show that the phase above T_S is still gradually changing with cycling. In particular, the ΔR-step at T_S decreases upon thermal cycling, gradually producing a more resistive phase above T_S.

3.4. Series 4 (runs 29–36)

After the previous cycles, the sample was warmed to 300 K, staying at room temperature for 20 days. A continuous increase of the electrical resistance was monitored during that period, showing relaxation towards saturation, with a final R increase of 40% (see [12]).

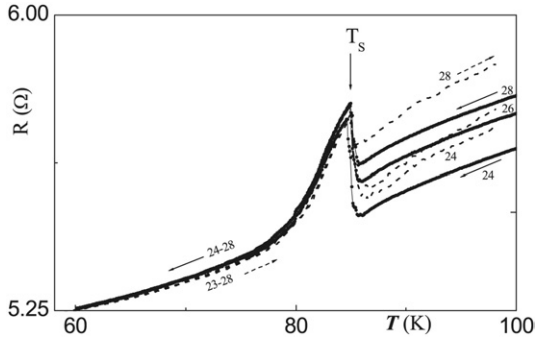

Figure 10. Temperature dependence $R(T)$ of $Gd_5(Si_{0.1}Ge_{0.9})_4$ in cooling runs 24–28 and heating runs 23–28 (dashed curve).

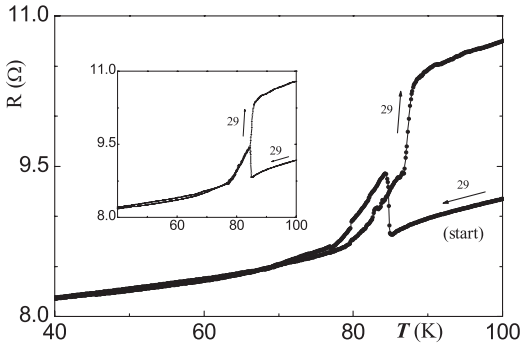

Figure 11. Temperature dependence $R(T)$ for $Gd_5(Si_{0.1}Ge_{0.9})_4$ in the 29th cooling and heating runs. The cooling run started at 300 K, after keeping the sample at room temperature for 20 days. The following heating run finished at 105 K. Inset: direct comparison of the cooling and heating curves, with a small shift in the temperature scale to make $T_S(\text{cooling}) = T_S(\text{heating})$.

The sample was then cooled to initiate a new series of 10–105 K thermal cycles (series 4; runs 29–36). Dramatic $R(T)$ differences (cooling versus heating runs) were immediately observed in the 29th thermal cycle, as shown in figure 11.

In cooling run 29 (from 300 K in this case) the $R(T)$ shape is still the same as in the previous runs (series 3, resistance peak at T_S and ΔR-step with large $dR/dT < 0$), but in the subsequent heating curve a totally different $R(T)$ curve emerges, with no resistance maximum at T_S. One observes instead a sharp increase of $R(T)$ just at T_S. This is better seen if we plot both $R(T)$ curves with a small shift in one of the T-scales ($\simeq$2 K, to account for ΔT_S), as shown in the inset of figure 11. The 29th heating run definitely switches the sample into a high-resistance phase just at T_S. This somehow resembles the effects observed in the 22nd thermal cycle (figure 8), which also started with cooling from 300 K.

In the following 10–105 K runs ($p = 30$–35) the shapes of the cooling and heating $R(T)$ curves become similar (figure 12) and essentially reflect the transition from a low-resistivity ($T < T_S$) to a high-resistivity phase (above T_S). Occasionally, a small peak reminiscent of the $R(T)$ behaviour in series 3 is still visible near T_S, suggesting a faint mixing of phases near T_S.

This systematic evolution to a definite high-resistive phase above T_S is essentially maintained in the subsequent thermal cycles (performed until $p = 50$).

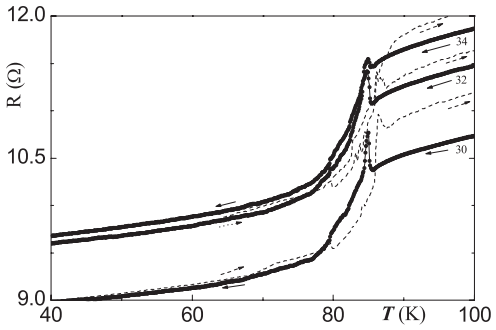

Figure 12. Temperature dependence $R(T)$ obtained for $Gd_5(Si_{0.1}Ge_{0.9})_4$ in thermal cycles 30, 32 and 34 (10–105 K). Heavy curves: cooling. Dashed curves: heating.

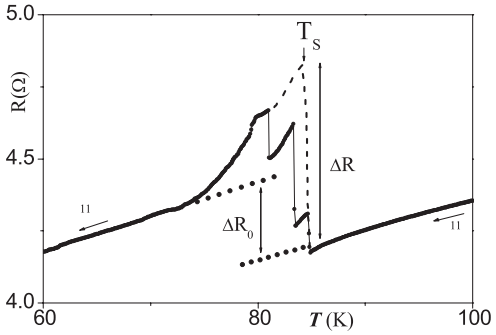

Figure 13. Temperature dependence $R(T)$ of $Gd_5(Si_{0.1}Ge_{0.9})_4$ in the 11th cooling run. The martensitic transition produces three discontinuous resistance steps (ΔR_1, ΔR_2, ΔR_3) for $T \leqslant T_S = 85.0$ K (solid curve). If these steps were all to occur at T_S, the result would be the dashed curve displaying a total ΔR increase ($\Delta R_1 + \Delta R_2 + \Delta R_3$) at T_S. A significant part of ΔR remains below the transition, in the form of residual resistance (ΔR_0; permanent defects).

4. Discussion

4.1. Initial thermal cycles

The initial splitting of the martensitic transition in three stages at slightly different temperatures T_i (runs with $p < 12$) is likely to be due to internal stresses and defects, locally preventing inter-slab sliding. The virtual reproducibility of each T_i reveals a memory effect, here associated with lattice defects. The transition-split in a few steps indicates that martensitic transformations initially occur independently in large sample regions. This is physically plausible, since such transitions are not driven by thermal fluctuations but by a suitable external parameter (see section 4.4), leading to inhomogeneous nucleation [14]. Upon thermal cycling, one expects progressive stress/strain accommodation and the thermodynamic transition point T_S is thus identified with the highest T_i observed.

The martensitic displacements also produce short-range disorder (srd) under cooling, since an extra ΔR_0 contribution appears in the residual resistance (figure 13). Previously, R_0 increases under thermal cycling were observed in $Gd_5(Si_xGe_{1-x})_4$ samples [15] and were associated with the production of microcracks. We notice that microcracks imply a change in the sample form factor and in R by the same multiplicative factor. Our results above T_S show virtually parallel $R(T)$ curves in different cycles (see figure 3(a)), putting an upper limit of

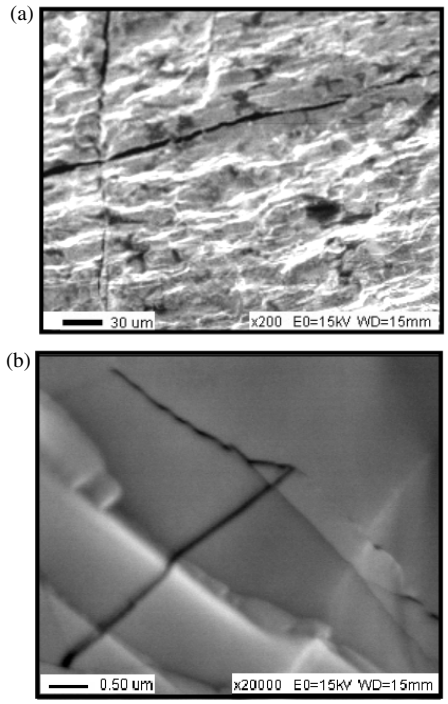

Figure 14. (a) SEM image showing microcracks with ∼600 nm width, observed on the surface of the $Gd_5(Si_{0.1}Ge_{0.9})_4$ sample used in this work (after 51 thermal cycles), (b) small microcracks with ∼50 nm width are also visible in other surface regions.

∼2% on the possible form factor changes, whereas the observed ΔR_0 demands 6% (figure 13). Therefore, the presence of microcracks in our samples (confirmed by SEM, figure 14) cannot explain most of the observed ΔR_0 changes. Conclusive evidence of the secondary role played by microcracks is given in the next section.

In the initial *heating runs* a resistivity excess already occurs over a restricted temperature range below T_S (figure 3(b)). This anomalous behaviour prompted us to re-analyse available powder x-ray diffraction data for a $Gd_5(Si_{0.1}Ge_{0.9})_4$ virgin sample taken from the same batch [8], as a function of temperature and encompassing the transition region. As shown in figure 15, the a, b and c lattice parameters (obtained from a Rietveld refinement) reveal a weak anomalous behaviour just below T_S. Above T_S these parameters stay constant, discarding long-range structural changes until room temperature. Lattice parameter constancy also prevails slightly below T_S, down to the lowest temperatures. Therefore, in the initial thermal cycles the (long-range) structural transformations are accomplished within a small temperature range below T_S, i.e. the so-called start and finish martensite (austenite) transition temperatures, M_s and M_f (A_s and A_f) [16, 17] are fairly close to each other in each case (cooling or heating), although a few degrees of thermal hysteresis exists ($M_s \neq A_s$, $M_f \neq A_f$).

4.2. Reproducible $R(T)$ behaviour within ΔT just below T_S

New effects suddenly appear in the 12th (heating) and subsequent runs, leading to a reproducible resistance behaviour $R_u(T)$ just below T_S (resistance excess; short runs 13–21 in figure 5(b)) and not displaying the previous three-step $R(T)$ structure. This indicates

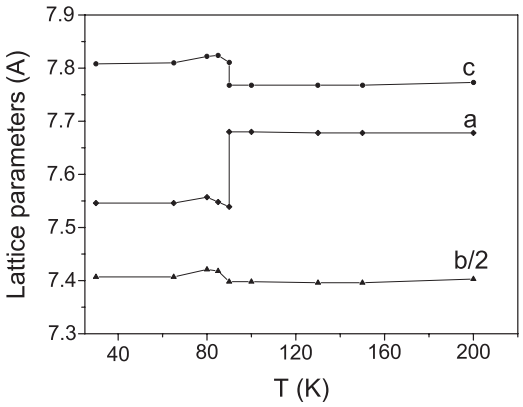

Figure 15. X-ray diffraction data of lattice parameters for $Gd_5(Si_{0.1}Ge_{0.9})_4$ compound as a function of temperature (4–300 K; from [8]). The points were taken under heating, after zero-field cooling the powder from 300 to 4 K.

the formation of a well defined and reproducible state just *below* T_S, whereas large differences (upon cycling) are observed in $R(T)$ outside the ΔT-range. Although higher resistance values just below T_S also appeared before ($p < 12$, section 3.1; see figure 3(b)), they were smaller and not reproducible. The new results indirectly indicate that significant microcracking did not occur under cycling, since the unavoidable changes in the sample form factor would immediately spoil the reproducible $R_u(T)$ behaviour. For the same reason one can say that, in the new regime, permanent srd is no longer produced when the sample cools through T_S. In addition, the $R(T)$ behaviour emerging in the 12th heating run cannot be attributed to a change in the temperature span of the previous thermal cycles (always covering the 10–300 K range; see figure 2).

The 'exact' $R_u(T)$ reproducibility just below T_S in the subsequent short runs (10–105 K) indicates a memory effect preserved by such moderate heating above T_S. In fact, the $R_u(T)$ reproducibility has been subsequently affected through a 10–300 K thermal cycle (see figure 8; 22nd run).

The reproducible $R_u(T)$ behaviour starts (under heating) with a sudden resistance increase at a characteristic temperature T_Δ, suggesting an avalanche-type transformation [14, 18] (see section 4.4). The R-values above T_S gradually rise and get closer to those observed within ΔT below T_S, as thermal cycling proceeds. Such resistance enhancement is not due to the formation of permanent defects during the transition, since no comparable increase subsequently appears in R_0, thus indicating a specific resistive mechanism *above* T_S (see section 4.3).

For the *cooling runs* ($p = 13$–21; figure 5(a)), the ΔT-range of 'local reproducibility' (starting at T_S) extends to lower temperatures with cycling (p), terminating at a kink-type anomaly at $T_\Delta(p)$, changing rapidly from first-order-like (figure 7(a)) to second order (figure 7(b)) under cycling. Below T_Δ, internal transformations still take place in the sample, as evidenced by the pronounced resistance decrease until a temperature $T^*(p)$ where thermal hysteresis disappears (figure 7). At lowest temperature the residual resistance increases under cycling, indicating a progressive enhancement of srd effects. However, since the sample always exhibits the same $R_u(T)$-values within ΔT near T_S, such srd effects are restricted to the low-temperature phase (more defective under thermal cycling; see below).

The $R_u(T)$ behaviour observed just below T_S under heating has similarities with the cap-resistance observed in memory-shape NiTi [19–21] and related alloys near the martensitic

transition [17, 22]. In these materials the effect was attributed to a *premartensitic* phase induced by a high dislocation density created by thermal cycling ($p \geqslant 11$ in [19]), producing high electrical resistance. However, such an anomalous phase appears above and not below T_S, which makes a similar explanation of our results problematic.

In our samples one should expect extra electron scattering near T_S, caused by lattice instabilities at the approach of the martensitic transition [23], namely hetero-phase fluctuations [24] associated with the simultaneous magnetic (FM $\rightarrow$ AFM) and structural (O(I) $\rightarrow$ O(II)) transitions at T_S, giving strong local disorder.

The difference in $R(T)$ under cooling and heating is here partially attributed to the differences in the nucleation and growth processes of the magnetic structures. In fact, the nucleation of an AFM phase ($q \neq 0$) out of an FM phase (under heating) can readily start inside the domain walls ($q \neq 0$), but the nucleation of an FM phase ($q = 0$) out of an AFM phase ($q \neq 0$) can be considerably delayed. Nucleation asymmetries may also exist for the structural O(I)/O(II) transformation, provided it is non-thermoelastic [26].

4.3. Reproducible $R(T)$ behaviour below T_S and its final evolution above T_S

With increasing number of cycles (figures 8 and 9), $R(T)$ becomes reproducible all the way below T_S, so short-range defects are no longer generated in the low-temperature phase. Preferential Si/Ge interchanges should occur upon thermal cycling [9, 27, 28], favouring migration of Si (Ge) atoms into (out of) the rigid slabs and thus an increase in the number of Ge–Si and Ge–Ge interslab bonds below T_S. The $R(T)$ reproducibility below T_S indicates that the bond pair composition (Si/Si, Si/Ge or Ge/Ge) is irrelevant for the electron scattering intensity. In contrast, systematic positive R-shifts continue to occur above T_S under heating. This suggests short-range disorder, but it completely disappears below T_S. Such $T > T_S$ effects could be associated with still unbroken Si–Si (or Si–Ge, Ge–Ge) pairs, i.e. incomplete martensite transformation under moderate heating above T_S. If so, the progressive enhancement of R above T_S (upon cycling) suggests increasing disruption of such residual bonds. This disruption should be favoured by the progressive formation of the weaker Ge–Si and Ge–Ge bonds [27, 28] under thermal cycling.

The processes referred to above saturate upon thermal cycling, leading to a stabilized high resistance phase above T_S. In a previous study on a $Gd_5(Si_{0.49}Ge_{0.51})_4$ sample [15], a stable high-resistance phase (called β'') was established for $p \geqslant 20$, but in our sample it appears for $p \geqslant 30$. The resistance enhancement was mainly attributed to the formation of twinned crystals during the O(I) $\rightarrow$ monoclinic transformation in such a particular compound [15]. One knows that twinning can evolve upon thermal cycling, ultimately leading to an extremely fine structure of twinned crystals [15, 29, 30], which could enhance electron scattering. In view of this, one cannot exclude the coexistence of residual-bond and twin-boundary electron scattering above T_S.

4.4. Magnetostructural transition dynamics

In this section we comment on the connections between our experimental observations and published theoretical work on the dynamics of martensitic transitions.

Generally the kinetics of martensitic transitions is not dominated by thermal fluctuations since the metastable minima are separated by high energy barriers and, consequently, they occur only under the influence of an external parameter (e.g. stress, magnetic field, temperature) which modifies the free-energy difference between high and low symmetry phases (athermal transitions) [26]. The system remains in a given configuration as long as the state corresponds

to a free-energy local minima, and it only jumps when the local stability limit is surpassed. Microscopically, the process usually evolves through a sequence of discontinuous steps or avalanches of the order parameter, with an associated energy dissipation and hysteresis [31].

The complex free-energy landscape is usually at the origin of mesoscale phase separation, leading to a polyvariant structure [25]. The path followed by the system is greatly influenced by disorder (dislocations, grain boundaries, vacancies, local composition, atomic boundaries, etc), which controls the distribution of energy barriers and nucleation processes. Thermal cycling is expected to change both the amount and the properties of disorder in the system, and thus the evolution of the phase transition characteristics. When the temperature rises above T_S any residual martensite plays an essential role in establishing the 'memory' from one cycle to the next. If the transformation is complete, only lattice defects can preserve such a memory effect and determine the system transition path in subsequent cycles. The evolution of the transformation kinetics can thus be understood as a learning process in which the system seeks an optimal path in the space of internal variables connecting the parent and martensitic phases. Such a path tends to avoid high energy barriers which separate local metastable states, in such a way that thermal cycling reduces metastability. After the learning period, a stationary state is reached and the transition is much more reproducible from cycle to cycle. In contrast, for the first cycles both the kinetics and microstructure in one cycle are not similar to the previous one and reproducibility is not achieved [14, 31].

These theoretical considerations provide a general physical picture to follow the global trends observed in our results in $Gd_5(Si_{0.1}Ge_{0.9})_4$, under successive thermal cycling. Nevertheless, many details in $R(T)$ require specific microscopic treatments, and for this we summarize a few topics worth particular attention.

All the available XRD structural information on virgin $Gd_5(Si_{0.1}Ge_{0.9})_4$ indicates that the lattice parameter changes are restricted to the immediate vicinity of T_S [8, 32]. However, the transport properties display a wealth of features outside such a region, with dramatic changes under extensive thermal cycling (even between consecutive cooling and heating runs). Since electron transport is mostly sensitive to sro effects (in the range of an electron mean free path), one concludes that important changes occur in point-defect and/or spin-disorder electron scattering during thermal cycling.

One should mention an important difference between the structural and magnetic sro components. For the structural part, one knows that these martensitic transitions are not induced by random thermal fluctuations, and so one does not expect significant (associated) structural fluctuations.

In contrast, the site spin-disorder fluctuations (sro) do not directly couple with the long-range structural features and should thus grow according to the specific magnetic interactions at play (RKKY in our case). Initial magnetic ordering occurs at $T_N = 128$ K in $Gd_5(Si_{0.1}Ge_{0.9})_4$, and so the magnetostructural transition ($T_S = 87$ K) takes place at a relatively high reduced temperature $t \simeq 0.7$, when significant spin-disorder is already expected. For a rough estimate, if we assume a mean field spontaneous magnetization dependence, $M(T)/M(0) \sim (1 - T/T_N)^{1/2}$, one gets $M/M(0) \sim 0.56$ at $T \sim T_S$. We believe that these strong srd magnetic effects (and the previously mentioned asymmetry in the nucleation of FM and AFM domains) play a relevant role in the $R(T)$ evolution under thermal cycling. In complement, preferential Si/Ge interchanges under thermal cycling [31] may add significant effects after many cycles.

New experiments and more extended research are still needed to clarify some of the microscopic issues raised in this work: for example, to directly check eventual microcracking (using electron microscopy) across the magnetostructural transition and up to room temperature, and to perform extensive thermal cycling under an applied magnetic

field. Also, detailed x-ray diffraction scans through the transition range, in successive thermal cycles and in high quality single crystals, are needed. However, such detailed experimental studies are beyond the scope of the present paper.

Acknowledgments

This work was supported by Acção Integrada E_32/09, through bilateral cooperation Porto-Zaragoza, by the Sapiens project POCTI/1999/CTM/36489 and project POCTI/CTM/42363/2001. Filipe Correia is thankful for a BIC grant (Project POCTI/36489) from Fundação para a Ciência e Tecnologia, Portugal. The financial support of the Spanish CICYT under Grant No MAT2000-1756 is also gratefully acknowledged. The authors gratefully acknowledge the collaboration of C Moreira Sá on the SEM measurements at CEMUP.

References

[1] Pecharsky V K and Gschneidner K A Jr 1997 *Phys. Rev. Lett.* **78** 4494
[2] Pecharsky V K and Gschneidner K A 1997 *Appl. Phys. Lett.* **70** 3299
[3] Pecharsky V K and Gschneidner K A 1997 *Adv. Cryog. Eng.* **43** 1729
[4] Morellon L, Sankiewicz J, Garcia-Landa B and Algarabel P A 1998 *Appl. Phys. Lett.* **73** 3462
[5] Pecharsky V K and Gschneidner K A 1999 *J. Magn. Magn. Mater.* **200** 50
[6] Pecharsky V K and Gschneidner K A 2001 *Adv. Mater.* **13** 683
[7] Pecharsky V K and Gschneidner K A 1997 *J. Alloys Compounds* **260** 98
[8] Morellon L, Basco J, Algarabel P A and Ibarra M R 2000 *Phys. Rev.* B **62** 1022
[9] Choe W, Pecharsky V K, Pecharsky A O and Gschneidner K A Jr 2000 *Phys. Rev. Lett.* **84** 4617
[10] Pecharsky A O, Gschneidner K A Jr, Pecharsky V K and Schindler C E 2002 *J. Alloys Compounds* **338** 126
[11] Pecharsky V K, Pecharsky A O and Gschneidner K A Jr 2002 *J. Alloys Compounds* **344** 362
[12] Sousa J B, Braga M E, Correia F C, Carpinteiro F, Morellon L, Algarabel P A and Ibarra M R 2003 *Phys. Rev.* B **67** 134416
[13] Sousa J B, Braga M E, Correia F C, Carpinteiro F, Morellon L, Algarabel P A and Ibarra M R 2002 *J. Appl. Phys.* **91** 4457
[14] Casanova F, Labarta A, Batlle X, Vives E, Marcos J, Manosa L and Planes A 2004 *Eur. Phys. J.* B **40** 427–31
[15] Levin E M, Pecharsky A O, Pecharsky V K and Gschneidner K A Jr 2001 *Phys. Rev.* B **63** 64426
[16] Otsuka R and Ren X 1999 *Intermetallics* **7** 511
[17] Wang W H, Chen J L, Gao S X, Zhan W S, Wen G H and Zhang X X 2001 *Appl. Phys. Lett.* **79** 1148
[18] Vives E, Ortín J, Mañosa L, Ràfols I, Pérez ŰMagrané R and Planes A 2001 *Phys. Rev. Lett.* **72** 1694
[19] Pelosin V and Riviere A 1998 *Metall. Mater. Trans.* A **29** 1175
[20] Uchil J, Mohanchandra K P, Kumara K G and Mahesh K K 1998 *Mater. Sci. Eng.* **251** 58
[21] Uchil J, Mahesh K K and Kumara K G 2002 *Mater. Sci. Eng.* **324** 419
[22] Zuo F, Su X and Wu K H 1998 *Phys. Rev.* B **58** 11127
[23] Vul D A and Harmon B N 1993 *Phys. Rev.* B **48** 6880
[24] Ren X, Otsuka K and Susuki T 1993 *J. Alloys Compounds* **355** 196
[25] Pérez-Reche F-J, Stipcich M, Vives E, Mañosa L, Planes A and Morin M 2004 *Phys. Rev.* B **69** 064101
[26] Pérez-Reche F-J, Vives E, Mañosa L and Planes A 2004 *Phys. Rev. Lett.* **87** 195701
[27] Choe W, Miller G, Meyers J, Chumbley C and Pecharsky A O 2003 *Chem. Mater.* **15** 1413
[28] Choe W, Pecharsky A O, Worle M and Miller G 2003 *Inorg. Chem.* **42** 1413
[29] Kartha S, Castan T, Krumhansl J A and Sethna J P 1991 *Phys. Rev. Lett.* **67** 3630
[30] Meyers J, Chumbley S, Choe W and Miller G J 2002 *Phys. Rev.* B **66** 12106
[31] Hardy V, Majumdar S, Crowe S J, Lees M R, Mck Paul D, Hervé L, Maignan A, Hébert S, Martin C, Yaicle C, Hervieu M and Raveau B 2004 *Phys. Rev.* B **69** 20407
[32] Holm A P, Pecharsky V K, Gschneidner K Jr and Rink R 2004 *Rev. Sci. Instrum.* **75** 1081